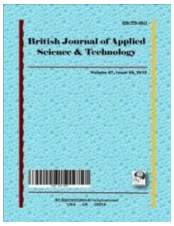

British Journal of Applied Science & Technology
8(5): 414-426, 2015, Article no.BJAST.2015.221
ISSN: 2231-0843

SCIENCEDOMAIN *international*
www.sciencedomain.org

Action of EM Disturbances on the Availability and Range of Indoor PLC Transmitters and Impact of Radiation on the Environment around Channel

Jamal Belkadid[1*], Ali Benbassou[1], Mohammed El Ghzaoui[1] and Achraf Liakouti[1]

[1]Department of Electrical Engineering, Sidi Mohamed Ben Abdallah University, High School of Technology of Fes, Laboratory of Transmission and Information Processing (LTTI), Team: CEM/TelecomsBP. 2427, Rte d'Imouzzer, Fes, Morocco.

Authors' contributions

This work was carried out in collaboration between all authors. Author JB designed the study, and wrote the first draft of the manuscript. All authors managed the analyses of the study and literature searches. All authors read and approved the final manuscript.

Article Information

DOI: 10.9734/BJAST/2015/16615
Editor(s):
(1) Chien-Jen Wang, Department of Electrical Engineering, National University of Tainan, Tainan, Taiwan.
Reviewers:
(1) Emodi Nnaemeka Vincent, Department of Technology, Management, Economics and Policy Program, Seoul National University, South Korea.
(2) Anonymous, Morocco.
(3) Vojko Matko, Faculty of Electrical Engineering and Computer Science, University of Maribor, Slovenia.
Complete Peer review History: http://www.sciencedomain.org/review-history.php?iid=1073&id=5&aid=8966

Review Article

Received 9th February 2015
Accepted 24th March 2015
Published 27th April 2015

ABSTRACT

The use of power lines for transmission of broadband data for applications such as Internet access or home automation, is certainly very attractive, but the problem of electromagnetic interference and radiated caused by these new systems. Risk of interference to radio reception is mainly approached in the frequency band ranging from 1 MHz to 30 MHz allocated to power line communication (PLC) and covers including HF.
The experimental study throughout this work show that the coupling factor has a strong dependence relative to the measurement location, to the topology of the electrical network and to a lesser degree, relative to the level of the load impedance. Thus, we made possible an estimate of the radiated field for a known injected signals. Experimental characterization of the indoor measurement also showed that the field values are dispersed; against for outdoor a proportional

**Corresponding author: E-mail: belkadid@gmail.com;*

decrease relative to the distance can be observed.
The different results permit to deduct a few orders of magnitude as well as some simple rules of use for minimizing exposure while allowing normal operation of the application level. In all cases, measured or simulated covered by the study, the required levels are met. In situ measurements show that human exposure to the electric field radiated by the PLC network is very small (< 1 V/m) compared to the reference limits.

Keywords: PLC network rate; PLC radiation; DAS; coupling factor; PLC; EMC standards.

1. INTRODUCTION

The experimental study throughout this work show that the coupling factor has a strong dependence relative to the measurement location, to the topology of the electrical network and to a lesser degree. To prevent pollution, the scientific community is trying to set standards [1-10] to prescribe a transmission power and transmission modes that meet the electromagnetic environment near or distant zone to these devices. As shown by [11-16], electromagnetic pollution is important in new HF switching mode measurements, so it thus appeared interesting to make measurements on PLC devices in operation to determine how radiation ranged relative to the proposed limits [17,18].

Experimental investigations are performed on typical energy lines. In section 2 we demonstrate the inadequacy of plane wave theory around PLC channel. Hence, we present in section 3 an approach for evaluating the transmission power of the PLC devices, while respecting the requirements of the dharmonized standard EN-55022 for conducted disturbances produced by any equipment connected to the power grid. The experiments designed to support the physical interpretations were mainly conducted within a specially equipped to obtain reproducible measurements. Indeed, the network model implanted Hall ICT laboratory may be, as appropriate, independent or connected to the general grid of the building. The test line is comprised of three conductors disposed randomly in a PVC conduit. Two conductors used to carry high frequency signal, the third conductor close precedents, may or may not be connected to the system ground.

The second part measures the radiation of EM field with a part of the electric power system of limited length to 8.5m will be discussed in section 4. Explored frequencies lie between 1 MHz and 10 MHz focusing injection signals produced by sinusoidal sources maintained and unmodulated. The radiated field is mainly characterized by the magnetic or electrical component measured at distances ranging from a few centimeters to a few meters from the power line.

Then the results will be extended to the case of the overall network of the room in order to highlight the increase in size of the tree and by connecting the local network to the core network of the building. We will establish the estimation of electric fields and proceed to a confrontation with the limits found in certain international standards.

2. INADEQUACY OF PLANE WAVE FOR PLC CHANNEL

The space around a radiating antenna can be divided into two regions: the near field and far field. For an antenna having a maximum dimension is small compared to the wavelength, the near field region is a region of induction, and the electric and magnetic fields store energy while producing little radiation. This stored energy is transferred periodically between the antenna and the near-field region in Fig. 12. This region extends from the induction antenna at a distance *R*.

$$R = \frac{\lambda}{10} \tag{1}$$

where λ is the wavelength.

There is no general formula for estimating the intensity of field region close to the small antennas field. You cannot make accurate for well-defined, eg. dipoles and monopoles sources calculations. In the case of antennas whose dimensions are large compared to the wavelength, the near field region comprises the induction of which extends over the distance R and is followed by a region of radiation. In the radiating near field, the field strength does not

necessarily decrease steadily unless it moves away from the antenna, since it may have an oscillatory character. In the area near radiation intensity of the electric field (*E*) and the magnetic field intensity (*H*) are interrelated according to the following formula:

$$\frac{E}{H} = Z_0 \qquad (2)$$

Power density *P* is calculated as follows:

$$P = \frac{E^2}{Z_0} = H^2 Z_0 \qquad (3)$$

Z_o is the intrinsic impedance.

Based on simulation results of [16], shown in Figs. 1-a and 1-b and the equation (3), the plane wave approximation is not very suitable for the case in view of the PLC frequencies used.

Simulations for the ratio *E/H* (Fig. 1-a) show that for a fixed frequency to 30MHz, the value Z_o varies depending on the distance in the near field and the plane wave approximation becomes valid only from a distance of 50m.

In the far field region, the field has essentially the character of a plane wave, ie. that the electric field vector is perpendicular to the magnetic field vector, and both are transverse to the direction of propagation.

The ratio between the intensity of the electric field and the magnetic field is constant at any point, in free space, it is equal to:

$$Z_0 = 377\Omega \qquad (4)$$

For a typical distance in an indoor environment (3 *m*), we see in Fig. 1-b for less than 40 *MHz*, the *E/H* ratio may be very different from the impedance of the vacuum.

We measured as shown in section 4, the vertical component of the electric field by replacing the antenna loop by a monopole antenna. The results in Fig. 2 show an underestimate of the true level of this electric field is possible. However, finding a significant dispersion of observed measurements, we note that the use of the plane wave approximation to express the electric field remains the most convenient. So, we will deduct the electric field from the measured magnetic field. Especially as the direct measurement of the electric field is subject to many other factors.

3. ACTION OF EM INTERFERENCES ON THE AVAILABILITY AND RANGE OF PLC MODEMS

3.1 Immunity of PLC Equipements

Problems related to immunity PLC beyond just the scope of this work because it was primarily to focus on the problems of issue. However, we can say that information about problems resulting from the operation of PLC devices or services in its environment are rare. At first sight, one might wonder if a radio transmitter can disrupt communication PLC. The answer here depends on the system in question, or rather the modulation used.

Broadband techniques, like Spread Spectrum, are very robust against interference [1]. Regarding OFDM, the signal is injected on multiple carriers at a time; the signal can be reconstructed by overlap even if it has been reduced on one or more carriers.

For immunity equipment PLC, the referenced standard is EN - 55024 on the ATI does not generally pose any particular problems for the latest generation of modems compared to other equipment covered by the standard. This standard specifies the degree of resistance equipment PLC disturbances present in its environment [2]. Indeed, this test involves injecting a carrier on the power modulated at 80 *%* of an amplitude level of 3*V* whose frequency ranges between 150 *kHz* and 30 *MHz* and is then superimposed on the carrier PLC.

3.2 Effects of Interference Produced by a Coupled Wave Radiation, Over Range of PLC Modems

In this section, we focus on the performance of PLC modems past generations in terms of throughput and robustness with respect to a disturbance generated by a radio transmitter in the frequency band [1-30 *MHz*].

The communication is performed according to the assembly of Fig. 3. The test circuit consists of two PLC modems connected to two computers for data transfer on the grid using the following configuration: take *E* (emitter) and taking *R* (receiver). A signal generator covering the frequency band [1-30 *MHz*] of *RF* amplifier and a

frequency band same amplifies the injected where the generator output signal is limited. An antenna for generating an *RF* disturbance by radiation or by injection to simulate the effect of a radio antenna in the vicinity of the PLC network.

We measure the throughput received versus flow transmitted using two modems of the same family. The measurement is performed under the effect of an *RF* interference at different frequencies depending on the power level. Immunity tests we performed on PLC modems new generation towards a carrier radiated disturbance centered in the band [1.6-30 *MHz*], showed a level of -10 *dBm* no problem. Indeed, these types of modems use a multicarrier modulation (OFDM) as that of the specification or HomePlug spread spectrum which exhibit good flow robustness point of view.

3.3 Effects of Interference Produced by a Coupled Wave Injection

Figs. 4 and 5 show the measurement results of immunity (or sensitivity) of the new generation of PLC modems (85 *Mbit/s* and 200 *Mbits/s*). The measurements are performed assess baths debit transmitted by the PLC network length L_C = 17 *m* as a result of variation in the level of *RF* interference frequency 4.4 *MHz*, 5.5 *MHz*, *11 MHz*, 13.5 *MHz*, 18 *MHz* and 21.5 *MHz* coupled network injection.

In Fig. 4, we see that the modems to 85Mbit/s has a substantially constant speed around 35 *Mbit/s* for lower interference levels of-22 *dBm* threshold. Beyond this value, modems become very sensitive and stops transmitting completely for a -15*dBm RF* disturbance. By cons, modems 200*Mbits*/s have low immunity to 85 *Mbit/s* modems. Sensitivities begin to increase from a level of -35 *dBm RF* interference (Fig. 5).

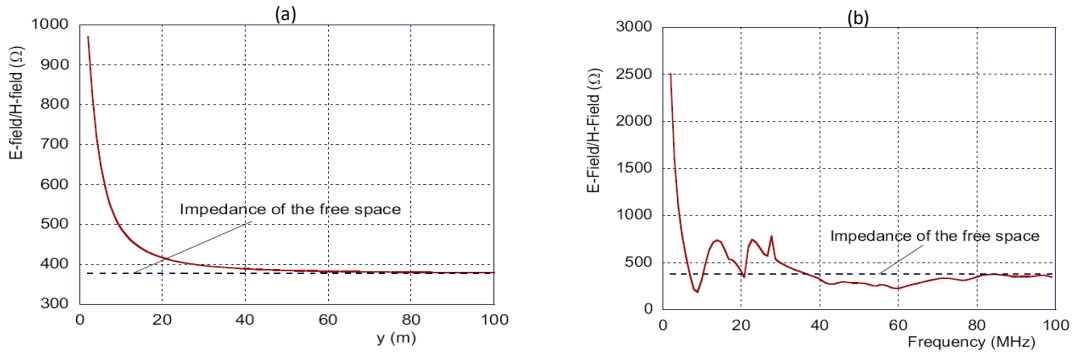

Fig. 1. Variation of the ratio *E/H* with distance for a fixed frequency of 30 *MHz* (a) & Depending on the frequency at a fixed distance of 3m from the PLC network (b)

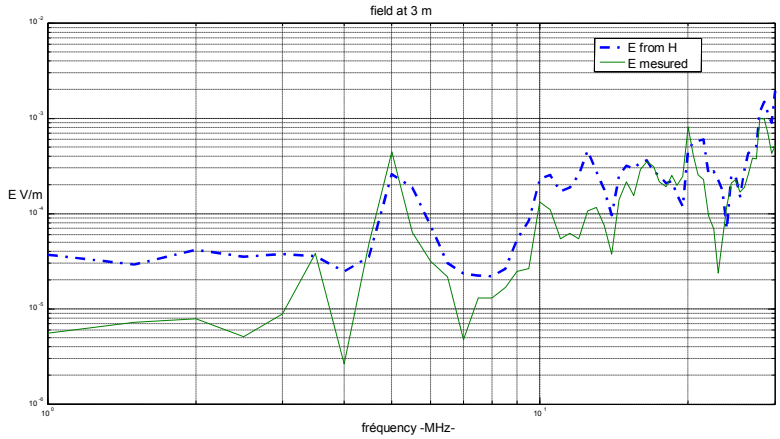

Fig. 2. Comparison between the vertical component and the total electric field estimated at 3*m*

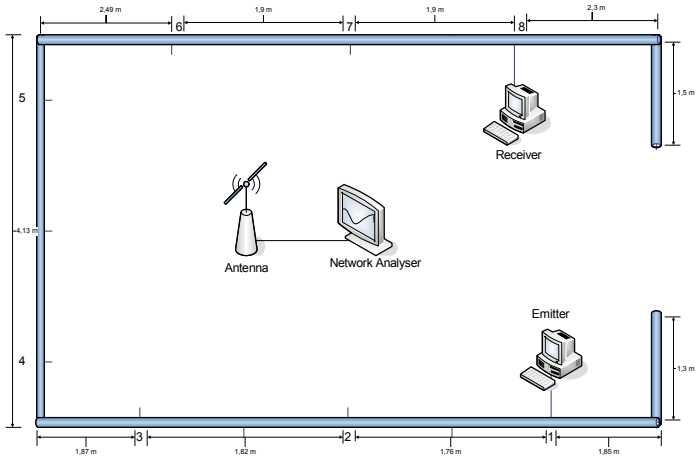

Fig. 3. Experimental PLC network

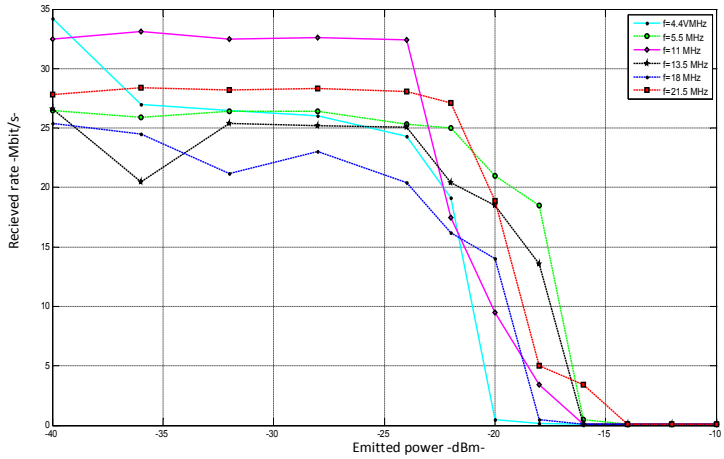

Fig. 4. Measurement of sensitivity modems 85 *Mbits/s* for *RF* interference in the band [4.4 *MHz* - 21.5 *MHz*]

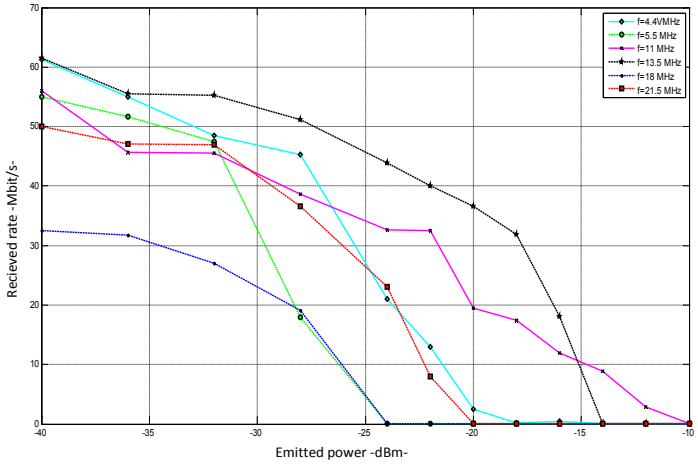

Fig. 5. Measurement of sensitivity modems 200 *Mbits/s* for *RF* interference in the band [4.4 *MHz* - 21.5 *MHz*]

4. EXPERIMENTAL CHARACTERIZATION OF PLC STRUCTURE RADIATION

The level of radiated field is a constant concern for possible disturbances in the functioning of other household appliances and services using the same frequencies (especially radio amateurs and military communications) or on the health of users of PLC [19].

A number of measurement campaigns aimed to characterize the point of view of the electromagnetic environment PLC then estimate the radiation equipment in operation became necessary. The following sections show the conditions under which they were made and the main results.

At first try to describe briefly the standardization work are for PLC. It is necessary to recall that the frequency band used by the PLC which runs up to 30 *MHz* in the band overlaps widely used by radio services (*HF* band) [20]. All these services are protected; the use of PLC shall in no case affect their operation. Thus, it is necessary to distinguish two types of normalization with the PLC broadband lines [21,22]:

- The first type involves equipment: Injection levels must not exceed limits set by the international CISPR 22 [23] standard.
- The second concerns the electromagnetic radiation caused by the use of low voltage network to the PLC with the aim that radiation does not cause disturbance in the reserved band for radio broadcasts.

For PLC systems, we must ensure reliable data transmission while maintaining their emission levels and interference within acceptable limits. Moreover, the grid is subject to external influences, which cause many disturbances. Electrical networks are viewed as open systems drivers, insufficiently protected.

Different work methods and describe how to implement the disruptive to apply in situ to assess the sources of disturbances and levels of past emissions analysis. In general, these studies follow already established standard [24-26].

Regarding the measurements of electromagnetic interference caused by PLC, we will define coupling factors $k_E\ (f)$ and $k_H\ (f)$, as that was established in [25], these parameters will allow us to characterize the electromagnetic behavior PLC network, regardless of the specific PLC signal, with respect to the voltage *U (f)* of the actually transmitted signal.

$$k_E(f)=\frac{E(f)}{U(f)} \qquad \left[\frac{1}{m}\right];$$
$$k_H(f)=\frac{H(f)}{U(f)} \qquad \left[\frac{A}{Vm}\right] \tag{5}$$

with equivalent in dB1/m:

$$k_{E\,dB}(f)=20.\log\left(\frac{E(f)}{U(f)}\right) \qquad \left[dB_{1/m}\right];$$
$$k_{H\,dB}(f)=20.\log\left(\frac{H(f)}{U(f)}\right) \qquad \left[dB_{A/Vm}\right] \tag{6}$$

We can define a factor, this time relative to the transmitted power of the injected signal k_P this factor is given by:

$$k_p(f)=\frac{E(f)}{\sqrt{P(f)}} \tag{7}$$

where P represents the difference between the power fed by the generator and the reflected power. In analogy to equation (3) can also be expressed by k_P:

$$k_{pdB}(f)=20\log(E(f))-10\log(P(f)) \tag{8}$$

As shown in equations (5), (6) and (7), this factor k_P is a function of frequency radiated and connects the voltage *U* transmitted respectively transmitted power *P*, the injected signal field.

Determining factors coupling therefore requires the measurement of the following parameters:

- The voltage *U* of the injected signal power *P* and the injected signal.
- The electric field (*E*) and magnetic (*H*) emitted.
- The distance between the measuring point and the nearest point of the electric network.

4.1 Scheme and Measurement Procedure

Measurements of coupling factors presented below were made according to the following scheme shown in Fig. 7, taking into account the magnetic field as a reference.

The presence of the main components of this circuit diagram is explained as follows:

- Generator: in our case, it is a signal generator covering the frequency band [9 *KHz*-3 *GHz*]. Marconi Instruments.
- *RF* - Amplifier: provides a good signal / noise ratio, the presence of an amplifier, covering well also the frequency band [1*MHz- 500 MHz*] can be used to amplify the signal injected in the case where the generator is limited Release. *Nucletudes* Systems (30 *W*) Inc.
- *Directional coupler*: it allows, during the injection of the signal to measure the power transmitted and the power reflected due to the impedance mismatch between the generator and *LV* network.
- *Balun*: we can inject the signal into the PLC online. It transforms the asymmetric voltage generator in an injectable symmetrical tension in the PLC online. The circuit of such a device is shown in Figure 10. In this figure, the essential elements of the device are the two coupling capacitors connected directly to the network and the limiter is designed to prevent surges in the measuring device.
- *HF* Receiver: for measuring, you can use either an *HF* receiver or spectrum analyzer. (ROHDE SCHWARZ 9 *KHz* - 3 *GHz*)
- *Network analyser* : as *HF* receiver (Agilent 30 *KHz* - 6 *GHz*)
- *Digital oscilloscope :* Tektronix DP04104 (1 *GHz*)
- *Antenna loop*: This is a measure of the magnetic field in *dBµA/m*. This value is then converted into electrical field equivalent *dBuV/m*. The antenna used is type *AH* Systems Inc covering the frequency range between 1 *kHz* and 30 *MHz (SAS 564)*.
- *Monopole antenna*: for measuring electric field. The antenna used is type *AH* Systems Inc covering the frequency range between 9 *kHz* and 40 *MHz (SAS 551)*.

Measurements of the coupling factor k_E were conducted on a laboratory pilot section of the network. The equations used to characterize various premises are not valid for a strictly scientific point of view. The conversion of the measured magnetic field values by using a loop antenna allows us to know the equivalent electric field by means of the equation (2). This is equivalent, as indicated in equation (9), to add to the value of 51.5 $dB_{v/A}$ measured magnetic field to thereby determine its electrical equivalent.

This value of 51.5 $dB_{v/A}$ is equal to $20 \bullet log\ (Z_o)$. This approximation is not yet valid in the case where it is in the far field region. This area depends on the dimensions of the antenna *D* (diameter of the loop) and the wavelength *λ* of the field. The agreement indicates that the far-field region starts from a critical radius *r* equal to the maximum values of *λ* and D^2/λ.

$$E_{dB\mu V/m}(f) = H_{dB\mu A/m}(f) + 51.5\,dB_{V/A} \qquad (9)$$

The Fig. 7 shows the coupling factor k_E measured according to the arrangement described in the assembly of Fig. 6. The measurements are made at 20 *cm* and 1.20 *m* and 3*m* from the injection point on a network segment PLC length L_C = 8.5 *m*. These measurement results show a low influence of the position on the measurement of this form factor despite the use of approximations of plane waves.

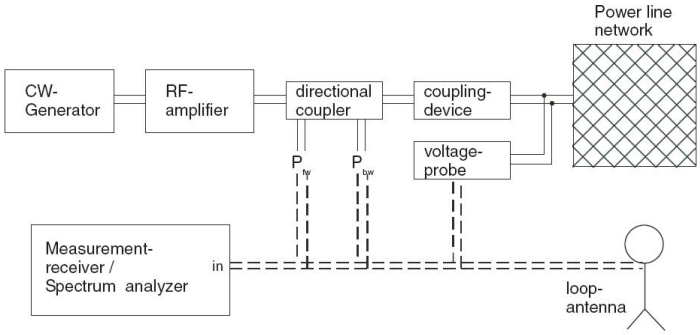

Fig. 6. Scheme of "automated" mounting with network analyzer

To maintain these approximations, we will adopt as a parameter of measure the factor k_H. The following sections describe the steps of the measurements made to determine this factor. Fig. 8 illustrates the coupling factor k_H in function of the position of measurement points, based on the model of the network portion of the laboratory.

Some measurement points have been placed in the room according to the distances recommended in Section 4. It shows that for the same frequency, gaps of 10 *dB* can be met. Fig. 9 shows the magnetic field in an indoor environment. A comparison between the radiated fields, resulting from the injection of PLC signals in compliance with the limits for Class B equipment to the power port by EN55022/CISPR22 standard.

In considering these figures, we can say that the resulting radiated field limits CISPR far beyond the Norwegian proposals and those of the BBC across the PLC band. Also, the radiated field resulting from the injection on the power port exceeds NB30 and UK MPT1570 over a wide band. While fields emitted remain below derived curves EN-55022 and FFC part15, almost over the entire band. We deduce thus that limit the radiated field derived from the EN-55022 appears to be the most sensible choice.

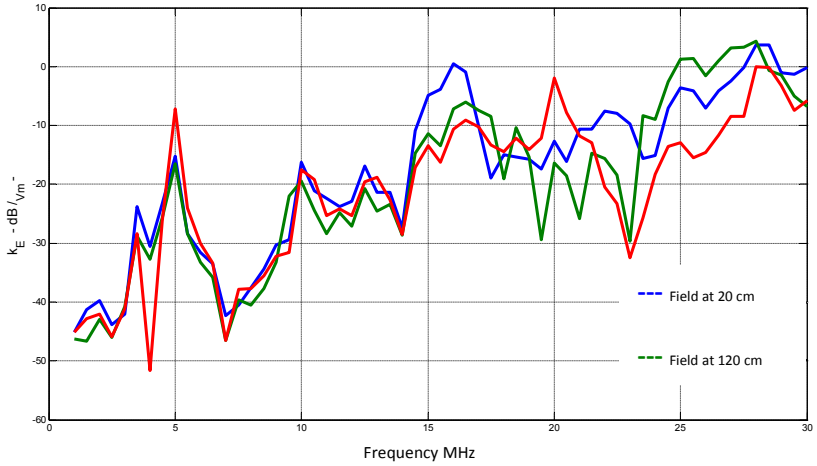

Fig. 7. Coupling factor k_E mesured at 20 cm, 1.20 *m* and 3 *m*

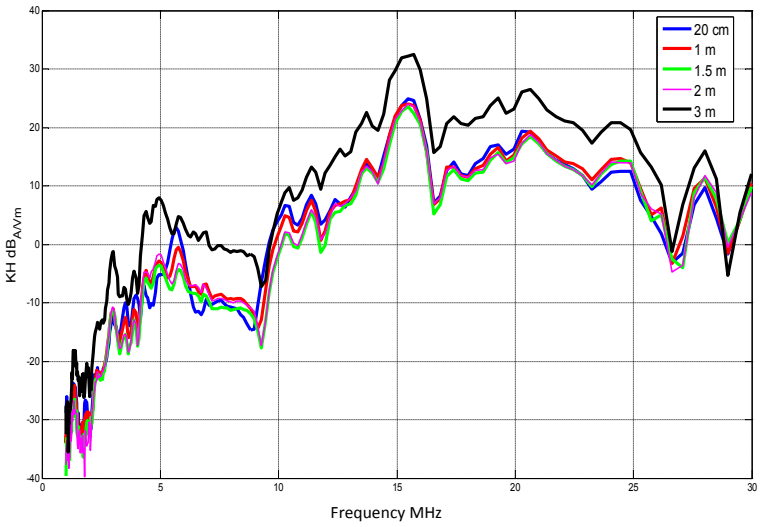

Fig. 8. Effect of the measurements location on the coupling factor k_H

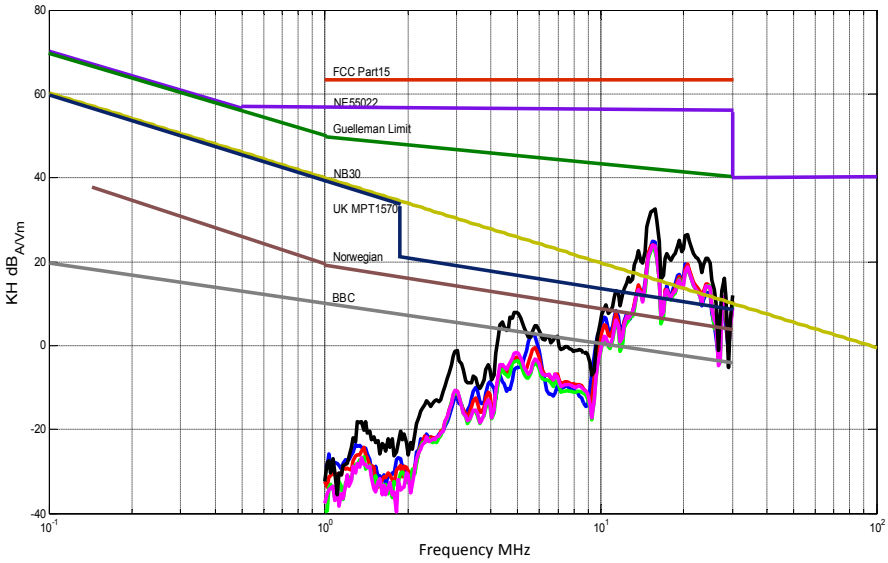

Fig. 9. Comparisons between the radiated fields resulting from the injection of PLC signals conforming to required limits and the various proposed standards

4.2 Radiations Measurements for real Network

A major concern caused by the PLC is the level of radiation that causes. It thus appeared interesting to make measurements on PLC devices in operation to determine how radiation ranged relative to the proposed limits. Also, to what extent these radiations could they affect the environment and the health of users rated the Specific Absorption Rate set by:

Electric Field *E(V/m)* in human tissues :

$$SAR = \frac{\sigma E^2}{\rho}$$

Current density *J (A/m²)* in human tissues:

$$SAR = \frac{J^2}{\rho\sigma}$$

Temperature variation in human tissues:

$$SAR = c_i \frac{dT}{dt}$$

- *J: densité de courant [A/m²], derived from magnetic or electric field.*
- σ *: conductivity S/m,* ρ*: density in kg/m*^{3}
- c_i*: Termal capacity in tissu J/(kg K).*
- *dT/dt: derivative of temperature in human tissues with respect to time*

To complete the tests in emissions maintained, a real digital transmission between PLC modems last generation, has been implemented to collect spectra radiated in the vicinity of the line installed indoor experiences. The scheme presented in Fig. 10 shows the measurement system on the radiation received from a global network of 17 *m* length embedded in the walls of the test site (Fig. 3).

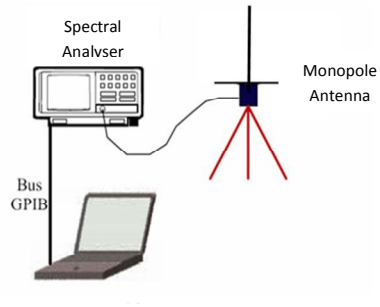

Fig. 10. Automated diagram installation

Thus, as shown in Fig. 10, the spectrum analyzer was used to scan all the PLC frequencies mode quasi-peak or peak to specification standards and to collect data for a post-treatment. At first, we started by measuring the current that flows in the feeding phase of the network on which the latest generation of modems using a multi-carrier transmission, according to the Home Plug standard, are connected.

In Fig. 11, the images are reproduced power spectra recorded on the line during a data

exchange stimulated by two computers. The spectrum analyzer connected to the line, is set to store maximum amplitudes captured during a measurement sequence. The filter (RBW) of the analyzer is successively four resolutions band equal to (10 *kHz*, 30 *kHz*, 100 *kHz* and 1 *MHz*).

These measures clearly indicate that in normal operation the power spectral density at the output of indoor modems -84 *dBm/Hz* and is close to the frequency band occupied by the signal ranges from 4 *MHz* to 20 *MHz*. Recall that the signal generator from a OFDM (Orthogonal Frequency Division Multiplexing), a technique designed to reduce the effects of interference encountered on the power line [26].

Fig. 12 shows the shape of the spectrum calculated from the three orthogonal components of the electric field and SAR identified by a monopoly to a distance of 20 *cm* and 120 *cm* from the nearest network PLC room network point total electric field equivalent laboratory. The metal plane interposed under the monopole antenna is to limit the direct coupling with the cable shield which encourages the extent that renders well captured by the antenna electrical component.

These curves show that the emission level is between 30 *dBuV/m* and 60 *dBuV/m*, in linear scale electric field with an amplitude of 0.03 *mV/m* and 1 *mV/m*. Radiation revealed by these figures is caused by the emission committed modems level. To evaluate the output power of modems, one may use the following relationship:

$$P_s = 10 \log R_{bw} + D_{sp} \qquad (10)$$

where P_S denotes the output power in *dBm* and D_{sp}, the power spectral density in *dBm/Hz*. Rbw is the width in *Hz* of the analysis filter. From equation (10), and considering a D_{sp} = -84 *dBm/Hz* deducted from statements of Fig. 11, the power engaged in a filter of width 10 *kHz* rise to achieve -44 *dBm*, which give a voltage of 56.98 *dBµV* across a load impedance of 50 Ω.

Successive measurements [27,28], varying the power level at the injection frequency 17.5 *MHz*, were made possible as shown by Fig. 6. Table 1 illustrates results of the effect of reducing the level of the input power, on the electric field radiation. Several observations can be made due to these measures. Firstly, the field decreases linearly with the injection level, which shows that a reduction of the field must go through a decrease of the emitted power. This would easily determine the power level to be injected to meet the limitation of radiation. The total component of the field was calculated from the measured other components. All values are summarized with their corresponding levels of injection in the table below.

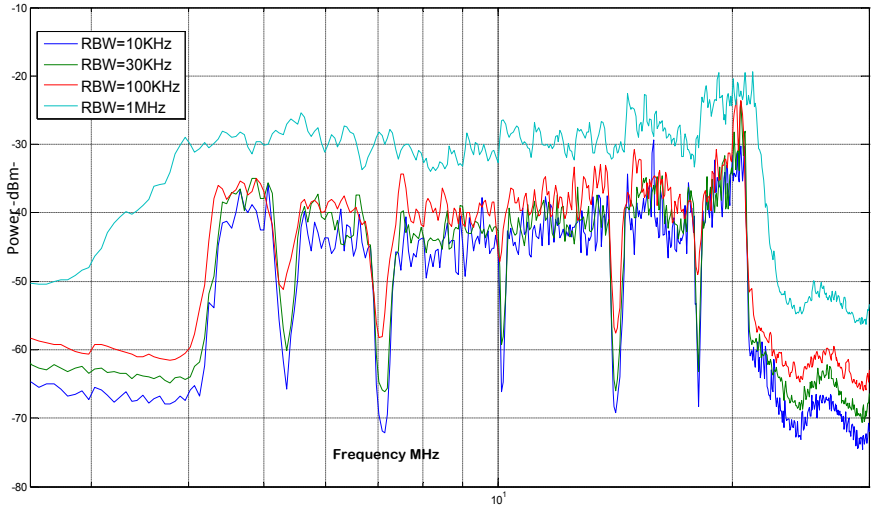

Fig. 11. Spectral envelope measured at the output of the PLC transmitter for different RBW setting of the spectrum analyzer (10 *kHz*, 30 *kHz*, 100 *kHz* and 1 *MHz*)

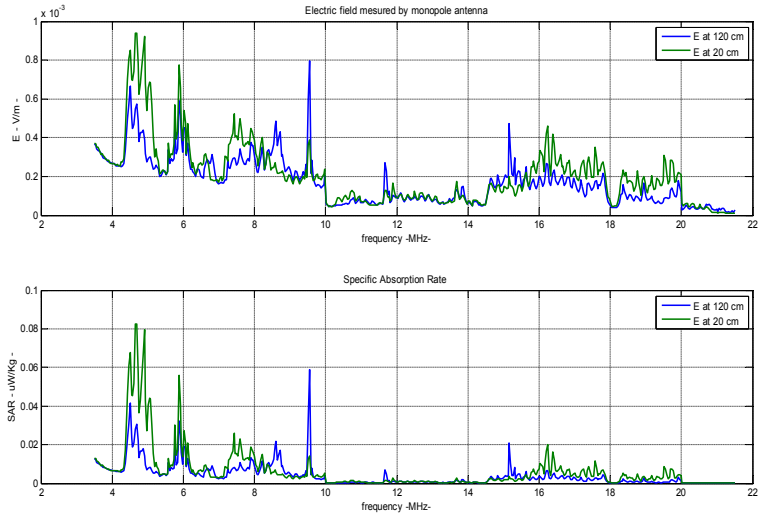

Fig. 12. Evaluation of SAR from total electrique field

RBW = 100 kHz, VBW = 3 kHz, SWT = 100 ms, attenuation level = 0 dB

Table 1. Field measured for different levels at the *CW* frequency 17.5 *MHz*

Injection level (*dBm*)	Componente *X* (*dBμV/m*)	Componente *Y* (*dBμV/m*)	Componente *Z* (*dBμV/m*)	Total field (*dBμV/m*)
30	67.39	67.11	66.36	71.75
25	62.02	62.17	61.74	66.75
20	57.37	57.00	56.35	61.70
15	52.37	52.01	51.30	56.69
10	46.76	46.53	45.79	51.15
5	38.32	37.16	37.47	42.45

Table 2. SAR limits as exiged by standards

Area of body	Average SAR (W/kg)	Integration time (minutes)	Average mass (g)
Full Body	0,08	6	Corps entier
Head and torso	1,6	6	1
Members (hand & legs)	4	6	10

4. CONCLUSION

The experimental study throughout this work show that the coupling factor has a strong dependence relative to the measurement location, to the topology of the electrical network and to a lesser degree, relative to the level of the load impedance. Thus, she made possible an estimate of the radiated field for a known injected signals. Experimental characterization of the indoor measurement also showed that the field values are dispersed; against for outdoor a proportional decrease relative to the distance can be observed.

The different results permit to deduct a few orders of magnitude as well as some simple rules of use for minimizing exposure while allowing normal operation of the application level. In all cases, measured or simulated covered by the study, the required levels are met. In the worst case observed (*f* = 4.8 *MHz to* 20 *cm* and *f* = 9.5 *MHz* to 120 *cm*), we quote:

- For a distance of 20 *cm* and an injection power of 56.24 *μW* (-45 *dBm*), the field strength is of the order of 0.95 *mV/m*, which is very low compared to the limit value 28 *V/m*. The SAR value is about 0.08 *μW/Kg*.
- For a distance of 1.20 *m* and an injection power of 56.24 *μW*, the field strength is of the order of 0.79 *mV/m*, which is very low

compared to the limit value cited above. The SAR value is about 0.06 $\mu W/Kg$.

In situ measurements show that human exposure to the electric field radiated by the PLC network is very small (< 1 *V/m*) compared to the reference limits (Table 2 above) given in [22]. The level of the SAR obtained by calculation is very low and rapidly decreases when the distance increases to the network.

COMPETING INTERESTS

Authors have declared that no competing interests exist.

REFERENCES

1. Marthe E. Power line communications: analyse de problèmes de compatibilité électromagnétique dans le domaine des courants porteurs en ligne. Thèse de doctorat, École Polytechnique Fédérale de Lausanne ; 2005.
2. El Ghzaoui M, Belkadid J, Benbassou A, ELBekkali M. Power Efficiency Improvement in CE-OFDM System with 0dB IBO for Transmission over PLC Network. Signal Processing International Journal (SPIJ), edition computer science journal. 2011;5(3):110-119.
3. Matko V, Milanović M. High Resolution Switching Mode Inductance-to-Frequency Converter with Temperature Compensation. Sensors. 2014;14(10):19242-19259.
4. Lars T, Joaquin J, al. Power Line Communications for Smart Grid Applications. Hindawi Publishing Corporation. Journal of Electrical and Computer Engineering. 2013;1-16.
5. Pascal, al. PLC Electromagnetic Compatibility Regulations. Devices, Circuits, and Systems. CRC Press. 2014;(Chapter6):169-186. ISBN 9781466557529.
6. Stanley H, Arun G. Power system relaying. 3rd edition. John Wiley and Sons. 2008;64-65. ISBN 0-470-05712-2.
7. Berger Lars T, Iniewski, Krzysztof. Smart Grid - Applicacions, Communications and Security. John Wiley and Sons; 2012. ISBN: 978-1-1180-0439-5.
8. Echelon Corporation. Echelon Announces ISO/IEC Standardization of LonWorks Control Networks. News release; 2008.
9. Martin H. Comparison of PLC G3 and Prime. IEEE Symposium on Power line Communication and its Applications. 2011;165-169. ISBN 978-1-4244-7751-7.
10. Lars BT, Andreas S, DanielS M. MIMO Power Line Communications: Narrow and Broadband Standards", chapter 10, EMC, and Advanced Processing. Devices, Circuits, and Systems. CRC Press; 2014. ISBN 9781466557529.
11. Stefano G, LeClare J, al. Narrowband Power Line Standards, chapter 11, Devices, Circuits, and Systems. CRC Press. 2014;270-300. ISBN 9781466557529.
12. ITU G.9903 ITU-T Web Page. Retrieved 6 March 2013.
13. Koren Y, Seri Y. Using LIN Over Power line Communication to Control Truck and Trailer Backlights. SPARC; 2007.
14. Xavier C. PLC Networks through practice Ed. Eyrolles; 2006. ISBN 978-2-212-11930-5.
15. Lars BT, Andreas S, Pascal P, Rensburg V, Janse P. MIMO Power Line Communications: Narrow and Broadband Standards. CRC Press. EMC, and Advanced Processing. Devices, Circuits, and Systems, chapter 1. 2014;3-38. ISBN 9781466557529.
16. MATKO, Vojko. Next generation AT-cut quartz crystal sensing devices. Sensors. 2011;5(11)4474-4482,
17. Norme. TS 50 437 Electromagnetic emissions from access powerline communications networks. CENELEC; 2004.
18. Marthe E, Rachidi F, Ianoz M, Zweiacker P. Indoor radia références. 193 TED emission associated with power line communications systems. Proc. 2001 IEEE Int. Symp. on EMC in Montreal, Canada, n.1, 2001;517-520.
19. Norme. IEEE 1528 Recommended Practice for Determining the Peak Spatial-Average Specific Absorption Rate (SAR) in the Human Head from Wireless Communications Device. Measurement Techniques.
20. Beeckman PA, van der Merwe J. Wired communication networks and EMC: An overview. Proc. 15th Int. Sym. On Electromagnetic Compatibility in Zurich, Switzerland. 2003;71-80.
21. Valperg P, Deventer V, Repacholi MH. Base stations and wireless networks: Raid frequency exposures and helth

consequences. Environmental Health Perspectives. 2007;115(3):416-424.
22. Deventer V, Simunic D, Repacholi MH. EMF Standards for human health. Hand Book of Biological effects of Electromagnetic Fields, 3rd Edition, Biological and Medical Aspects of EM Field, Ed. Barnes & Greenebaum. 2007;277-292.
23. Deventer V, Foster K. Risk assessment and risk communication for electromagnetic Fields. Chapter in Book of the Role of Evidence in Risk Characterisation, Edition Wiedemann and Schütz, WILEY-VCH. 2008;13-24.
24. IEEE EMC Magazine. EMC Standards Activity. 2014;3(4):90.
25. Gebhardt M. Radio disturbance characteristics - method of measuring the coupling factor of power line installations. PLC Forum Regulatory Working Group in Paris, France; 2000.
26. ElGhzaoui M, Belkadid J, Benbassou A. Peak to Average Power Ration Reduction in OFDM System Using Constant Envelope for Transmission via PLC Channel, International Review on Computers and Software (I.RE.CA.P.). 2013;3(5):267-272.
27. LeClare J, Niktash A, Loginov V. How a standard is born: IEEE P1901.2 for narrowband OFDM PLC Smart Grid Solutions, Maxim Integrated; 2013.
28. Mescco A, Pagani P, Ney M, Zeddam A. Radiation Mitigation for Power Line Communications Using Time Reversal. Journal of Electrical and Computer Engineering. Paper ID 402514; 2013.

Peer-review history:
The peer review history for this paper can be accessed here:
http://www.sciencedomain.org/review-history.php?iid=1073&id=5&aid=8966